DOI: 10.5604/01.3001.0010.4596

METHODS OF SMALL CAPACITANCE MEASUREMENT IN ELECTRICAL CAPACITANCE TOMOGRAPHY

Waldemar Smolik, Jacek Kryszyn, Tomasz Olszewski, Roman Szabatin
Warsaw University of Technology, Faculty of Electronics and Information Technology, The Institute of Radioelectronics and Multimedia Technology, Nuclear and Medical Electronics Division

Abstract. *The paper presents the main methods of small capacitance measurement used in electrical capacitance tomography: the AC method with a sine wave excitation and the charge-discharge method with square wave excitation. Construction of synchronous detector for both circuits was discussed. A modified "charge-discharge" method was presented.*

Keywords: capacitance measurement, AC method, charge-discharge method, electrical tomography

METODY POMIARU MAŁYCH POJEMNOŚCI W ELEKTRYCZNEJ TOMOGRAFII POJEMNOŚCIOWEJ

Streszczenie. *W artykule przedstawiono główne metody pomiaru małych pojemności stosowane w elektrycznej tomografii pojemnościowej: metodę częstotliwościową z pobudzeniem za pomocą fali sinusoidalnej oraz metodę „ładuj-rozładuj" z pobudzeniem za pomocą fali prostokątnej. Przedstawiono budowę detektora synchronicznego dla obu układów. Zaprezentowano również modyfikację metody „ładuj-rozładuj".*

Słowa kluczowe: pomiar pojemności elektrycznej, metoda częstotliwościowa, metoda „ładuj-rozładuj", tomografia elektryczna

Introduction

The electrical capacitance tomography allows to obtain a three-dimensional distribution or two-dimensional cross-section of the distribution of electric permittivity in the examined volume surrounded by the electrodes of capacitance sensor [4, 9]. An image of permittivity distribution is reconstructed by numerically solving the non-linear inverse problem, where the measurement data are the values of mutual capacitance of electrodes surrounding the examined volume [8].

Because of the problems associated with measurement of very small capacitance, the number of electrodes and hence the number of measurements is limited, thus the inverse problem is undetermined. A small number of measurements decides on the poor spatial resolution of this imaging technique [10].

Increasing the spatial sampling by increasing the number of electrodes is not possible due to the very small values of the mutual capacitance of electrodes of a tomographic sensor, of the order of femtofarads [14]. Reducing the area of electrodes while increasing the number of electrodes can't be compensated by increasing the height of electrodes due to the loss of resolution in an axis perpendicular to the plane of tomographic cross section. A change in the permittivity in a small volume results in a very small change in capacitance of the order of few femtofarads for the adjacent (neighboring) electrodes and a fraction of femtofarad for opposite electrodes (Fig. 1, Fig. 2). Wide measurement range, from picofarads for the neighboring electrodes to fractions of femtofarads for the opposite electrodes (Fig. 3), is a vital problem in the design of the measuring system.

Capacitance measurement circuits for electrical capacitance tomography should: have good linearity, be shielded to remove the effect of external electric field, be insensitive to the parasitic capacitance to ground and generate little noise. There are different methods of capacitance measurements, depending on the value of the measured capacitance, precision and speed. The methods can be divided into the following groups: DC circuits (charging capacitor using a constant voltage or current), RC, IC or LC oscillators in which the capacitance is converted to frequency, synchronous demodulators or synchronous dual-port bridges [1]. DC method (capacitor charging with direct current) can be realized by means of few elements, but at the expense of temperature drift and sensitivity to noise. Resonance circuits can cover a wider range of capacitance values than DC circuits but are sensitive to a parasitic capacitance and noise. The most suitable circuits for capacitance tomography are the dual-port synchronous demodulators, because of their high accuracy and immunity to parasitic capacitance.

The capacitance of coaxial cables that are used to connect the electrodes of tomographic sensor to the transmitting and receiving circuit, is a load of the order of 60 pF/m. The parasitic capacitance of analog CMOS transistors used to switch the electrodes is about 8 pF. The external screen of the probe, protecting against external electric field (signal interference), is an additional load, which capacitance value can reach several tens of picofarads. Due to the large total value of parasitic capacitance of about 150 pF, which is several orders greater than the measured capacitance, which value is in the range from about 1 pF for adjacent electrodes to about 1 fF for opposite electrodes, immunity of the measuring system to the parasitic capacitance is very important [14].

Among several proposed in the literature methods of capacitance measurement, two methods can be distinguished in capacitance tomography: frequency or AC method with sinusoidal excitation and charge-discharge method with square wave excitation. These two methods are used in most modern systems for capacitance tomography.

1. AC method

In the frequency or alternating current method (AC method) a sine wave is used as the excitation signal [15]. The sinusoidal excitation is applied to the capacitance connected in series.

The first stage of the receiver is an alternating signal amplifier (AC amplifier). Application of an amplifier with programmable gain ensures the maintenance of the amplitude of the output signal at the high level for a wide range of capacitance values. The signal from the amplifier is demodulated in the next stage of measurement channel using the rectifier [13] or phase-sensitive detector [4, 5], and smoothed using a low pass filter. Phase synchronization allows accurate measurement of signal amplitude, even when the signal is disturbed by broadband Gaussian noise or uncorrelated interference.

A block diagram of the AC measurement circuit is shown in Fig. 4. A generator of sinusoidal wave:

$$u_G(t) = U_{GEN} \sin(wt) \qquad (1)$$

is a source of alternating current flowing through the capacitance C_X connected in series to the generator. The first stage of the receiving circuit is an operational amplifier with feedback loop in the form of parallel connection of the capacitance C_F and the resistance R_F, which converts the alternating current into a voltage signal given by the formula:

$$U_{AC} = U_{GEN} \frac{j\omega R_F C_X}{1 + j\omega R_F C_F}, \quad (2)$$

where ω is an angular frequency of sinusoidal excitation. If the time constant $\tau = R_F C_F$ is large and the excitation frequency f is high (for example $R_F = 1$ MΩ, $C_F = 6{,}8$ pF, $f = 1{,}5$ MHz), the equation (2) simplifies to the form:

$$U_{AC} = U_{GEN} \frac{C_X}{C_F}. \quad (3)$$

The amplitude of the sinusoidal signal is proportional to the measured capacitance.

Demodulation of the sinusoidal signal from the AC amplifier takes place in the second stage of the measuring system consisting of a phase locked loop and low pass filter. Sinusoidal signal:

$$u_{AC}(t) = A \sin(\omega t + \alpha), \quad (4)$$

where α is the delay introduced by the measured impedance and the amplitude is given by the formula:

$$A = U_{GEN} C_X / C_F, \quad (5)$$

is multiplied by the reference signal:

$$u_R(t) = B \sin(\omega_R t + \beta), \quad (6)$$

what gives at output (after using the formula for the product of sines):

$$u_D(t) = \frac{AB}{2} \begin{bmatrix} \cos\left[(\omega - \omega_R)t + \alpha - \beta\right] - \\ \cos\left[(\omega + \omega_R)t + \alpha + \beta\right] \end{bmatrix}. \quad (7)$$

If the transmitter and receiver are synchronized ($\omega_R = \omega$), in the signal at the multiplier output:

$$u_D(t) = \frac{AB}{2}\left[\cos(\alpha - \beta) - \cos\left(2\omega t + (\alpha + \beta)\right)\right] \quad (8)$$

the DC component will be present. Additionally, if the signals are in phase, that is $\alpha = \beta$, the voltage at the multiplier output takes the form:

$$u_D(t) = \frac{U_{GEN} C_X B}{2C_F}\left[1 - \cos(2\omega t + 2\alpha)\right]. \quad (9)$$

A low-pass filter which is the last part of the receiving channel allows to obtain a constant signal with value directly proportional to the measured capacitance.

Application of synchronous detector, which is functionally equivalent to a band-pass filter, significantly improves performance of the measurement circuit because of the extremely narrow band filtration.

AC method is immune to parasitic capacitances. Parasitic capacitance C_{S1} is just a load of the sine wave generator and does not affect the measurement. From the driving electrode, parasitic capacitance is supplied from a source with very low internal resistance, so it has no effect on the potential at measured capacitance. The parasitic capacitance C_{S2} does not affect the measurement because it is maintained at virtual ground by the operational amplifier. The voltage accumulated on the parasitic capacitance is very small and its effect on the measurement is very small.

In some applications of electrical capacitance tomography, when the medium is a mixture of dielectric and conductive materials, it is important to measure not only the permittivity but also the conductivity of the medium. Capacitance measurement by synchronous demodulation can be modified to obtain the value of the impedance in the form of a module and phase. For this purpose, the quadrature modulation is applied using two orthogonal signals:

$$u_{R1}(t) = B \sin(\omega_R t + \beta), \quad u_{R2}(t) = B \cos(\omega_R t + \beta). \quad (10)$$

If we assume that the transmitter and receiver are synchronized, so the reference frequency is equal to the excitation frequency $\omega_R = \omega$, the multiplication of the output signal from the measured impedance with the reference signals gives respectively:

$$\begin{aligned} u_{D1}(t) &= \frac{AB}{2}\left[\cos(\alpha - \beta) - \cos\left(2\omega t + (\alpha + \beta)\right)\right] \\ u_{D2}(t) &= \frac{AB}{2}\left[\sin(\alpha - \beta) + \sin\left(2\omega t + (\alpha + \beta)\right)\right] \end{aligned} \quad (11)$$

If the reference signal is in phase with the excitation, so $\beta = 0$, after the application of low pass filters in each channel, the real part and the imaginary part of the signal will be obtained:

$$u_{D1}(t) = \frac{AB}{2}\cos(\alpha), \quad u_{D2}(t) = \frac{AB}{2}\sin(\alpha), \quad (12)$$

where α stands for the delay introduced by the measured impedance. Impedance modulus and phase shift can be determined using the formulas:

$$\frac{AB}{2} = \sqrt{U_{D1}^2 + U_{D2}^2}, \quad (13)$$

$$\alpha = \arctan\frac{U_{D2}}{U_{D1}}, \quad (14)$$

Quadrature method allows to get information about the measured impedance of the medium (amplitude and phase), but requires an application of a double channel demodulator.

The disadvantage of the AC method is relatively low speed of measurements, resulting from the low-pass filter cutoff frequency. In one of the reported solutions [15] the low-pass filter cutoff frequency is equal to 5 kHz, when the reference frequency is equal to 500 kHz, which gives measurement time of single capacitance equal to about 200 µs. In the case of 120 measurements for a sensor with 16 electrodes and single-channel measurement, the time of measurement of data for one picture is about 24 ms. This gives speed of image registration of about 41 frames per second.

In the case of multi-channel measurement with one driving electrode and a number of measurement electrodes the time of measurement of data for one image is 3.2 ms. This gives the frame rate equal to about 312 frames per second.

2. Charge-discharge method

In the charge-discharge method [5, 9], a transmitter circuit connected to the driving electrode generates a square wave. The circuit connected to the receiving electrode integrates the current pulses during repeated cycles of charging and discharging of the capacitor. Charging and discharging phases are accomplished through synchronous switching of stimulating and receiving circuits. At the receiver the two integrators are provided, one of which sums up the charging current pulses and the second sums up capacitor discharging current pulses. After summing of multiple pulses by both integrators, a fixed voltage level is settled at their outputs, with approximately equal absolute value but opposite sign. Differential processing of signals from both integrators using instrumentation amplifier doubles the value of the measurement signal.

Excitation consist of passing unipolar or bipolar square wave on the driving electrode. Measuring electrodes are virtually grounded, which allows simultaneous measurement of $n - 1$ capacitances, where n is the number of electrodes in the sensor.

Charge-discharge capacitance measurement circuit in differential configuration is shown in Fig. 5. One terminal of measured capacitor C_X is connected to a source of a square wave. The transmitter consists of two analog switches which synchronously switch between two voltage levels U_{T1} and U_{T2}. The other terminal of the capacitor C_X is connected to the pair of integrators selected by the switches controlled synchronously with the transmitter switches. Both integrators are current-voltage converters constructed using an operational amplifier.

Application of operational amplifier in the construction of integrators causes that the output terminal of measured capacitance is maintained at a potential very close to zero. The driving signal in the form of a square wave and the synchronous switching of integrators causes that the capacitance C_X is periodically charged and discharged. Let's assume, that the levels of a symmetrical square wave are respectively equal to: $U_{T1} = -U_T/2$ and $U_{T2} = U_T/2$. The amount of the charge transferred during a voltage jump from level to level is given respectively by the formula:

$$\Delta Q_1 = U_T C_X, \quad \Delta Q_2 = -U_T C_X. \tag{15}$$

The cyclic charging and discharging of the capacitor C_X at a frequency f causes the flow of current in both integrators with an average value respectively equal to:

$$I_1 = fU_T C_X, \quad I_2 = -fU_T C_X. \tag{16}$$

In a real system the typical values of voltage U_T are in the range from 10 to 15 V. The typical values of frequency f are in the range from 1 to 3 MHz. The measured capacitance C_X is in the range from 20 fF to 5 pF for most tomographic probes. Let's assume that the voltage amplitude of excitation waveform U_T is equal to 12V, the driving frequency f is equal to 1.5 MHz and the value of measured capacitance C_X is in the range from 0.01 pF to 2 pF. The charge Q_X determined from equation (15) is in the range from 0.12 pC to 24 pC. So small value of the charge is comparable to or even less than the value of charge injection for most semiconductor analog switches, ranging from 1 pC to 30 pC. Average value of current I_X given by the formula (16) equals from 0.18 μA to 36 μA. Exciting square wave U_A is distorted mainly by the resistance of the source and parasitic capacitances. Raising and falling of the signal last tens of nanoseconds, thus the charge Q_X is transferred in time period of about 20…50 ns with the mean value of the current equal from 3.4 μA to 0.69 mA.

Two integrators convert the current to voltage by a scaling factor determined by the value R_{FB} of resistance in the integrator feedback loop. The capacitor C_{FB} in feedback loop is charged by successive current pulses, but in the meantime it discharges through the resistor R_{FB}. The output value stabilizes when the currents that charge and discharge feedback capacitance C_{FB} compensate each other (Fig. 6). The voltage at the integrators output tends asymptotically to a value of, respectively:

$$U_1 = -fU_T C_X R_{FB}, \quad U_2 = fU_T C_X R_{FB}. \tag{17}$$

Voltage addition is performed in a last element of the receiving channel using an instrumentation amplifier with differential input and programmable gain K. The instrumentation amplifier gives at the output almost constant voltage of average value:

$$U_{OUT} = 2KfU_T C_X R_{FB} \tag{18}$$

directly proportional to the measured capacitance. In the case of measurement of a small capacitance it is necessary to increase the gain, which can be achieved by increasing the excitation voltage U_T, increasing the frequency f or increasing the gain of the integrator by changing R_{FB} or increasing the gain K of differential stage.

Gain adjusting by increasing the resistance in the feedback loop of the integrator causes a simultaneous increase of the time constant of voltage settling what has an impact on the measurement time. The approximately constant voltage U_1 and U_2 have a low variable component in the form of ripple (Fig. 6) resulting from the process of charging and discharging of capacitance C_{FB} [11]. Single pulse changes the output voltage by value equal to:

$$\Delta U_1 = -U_T C_X / C_{FB}, \quad \Delta U_2 = -U_T C_X / C_{FB} \tag{19}$$

respectively for the integrator summing the charging current pulses and the integrator summing the discharging current pulses. Voltage pulses ΔU_1 and ΔU_2 arises in different moments, thus the ripple signal is transmitted by a differential amplifier with gain K. The ratio of the ripple amplitude to the average value of the signal depends on the time constants of the integrators, but does not exceed a maximum value:

$$\frac{\Delta U_{OUT}}{U_{OUT}} = \frac{1}{2fR_{FB}C_{FB}}. \tag{20}$$

This ratio depends on the components in the feedback loop R_{FB} and C_{FB}, and in the real conditions is from about 1/100 to about 1/1000. This means that the charge-discharge circuit produces a signal with a significant ripple component, with a signal-to-ripple ratio typically in the range 40 ÷ 60 dB.

To minimize the impact of ripple, a large time constant $\tau = R_{FB}C_{FB}$ should be selected. When the measured capacitance value C_X becomes smaller, the resistance R_{FB} in the feedback loop must be increased in order to achieve a measurable signal at the output. The value C_{FB} should be chosen as a compromise between the magnitude of the amplitude of the ripple signal and the measurement time.

A large capacitance value C_{FB} increases the time constant $\tau = R_{FB}C_{FB}$ and minimizes the ripple signal, but it requires an increased number of charging and discharging pulses. A large number of current pulses increases the measurement time and is not acceptable in high-speed data acquisition. To achieve optimum results the elements R_{FB} and C_{FB} in the feedback loop should be programmatically switched, according to the range of a measured capacitance.

In addition, to obtain a correct average value of voltage, it is necessary to filter the signal before sampling of the signal by the analog-to-digital converter. Band-stop filter for ripple frequency can be used. Another method might be to increase the sampling rate of A/D converter and digital filtering by averaging.

Charge-discharge method is insensitive to parasitic capacitances. The main problem of the circuit is a charge injected by the analog switches used for signal modulation [3, 6]. The example of circuit implementation is described in [2].

To achieve steady state on the integrator outputs some minimal number of pulses is required. This number depends on the value of the measured capacitance and may be approximately constant when switching elements in the feedback loop of the integrators. For the driving frequency equal to 1 MHz and 40 pulses, time of one capacitance measurement equals 40 μs plus conversion time, which for high-speed converters is less than 1 μs. In the case of 120 capacitance values for a sensor with 16 electrodes and single-channel measurement, the measurement time of the data for one image is about 4.8 ms. This means the speed of image acquisition of about 208 frames per second. In the case of multi-channel measurement with one driving electrode and many measurement electrodes, the measurement time of the data for one image is 0.64 ms, which gives about 1562 frames per second.

3. Switch-less charge-discharge circuit

The basic problem that occurs in the charge-discharge circuit is the effect of charge injection of the analog switches. Due to the discrepancy of this parameter between the switches applied in the circuit the charge injected to both integrators does not cancels at differential stage of the measuring amplifier. The zero level is shifted. One possible solution could be to replace the analog switches by diodes in a current rectifying configuration.

Replacement of the switch by the diode in classic charge-discharge circuit will not bring the expected results due to the position of the switch at the input of the system. A much better solution turns out to be the application of the active rectifier circuit with the diode in the feedback loop of the integrator. To sum charging and discharging pulses one operational amplifier can be used with the diode splitter configuration (Fig. 7).

Switch-less charge-discharge circuit was presented in [7, 12]. The circuit works on the same principle as in the classical charge-discharge method. The measured capacitor is sequentially charged and discharged and the charging and discharging current pulses are integrated respectively in two parts of feedback loop of the integrator.

The circuit consists of a square wave generator connected to the driving electrode and the demodulator connected to the measuring electrode. The electrodes of the tomographic sensor are connected to the transmitter and receiver via the analog switches or multiplexer. A square wave with a frequency of 1 MHz and amplitude of 10 V is given on the driving electrode. The receiver, connected to the sensing electrode, consists of a preamplifier and an integrator in a configuration of an active rectifier.

In the circuit there is only one integrator which has two feedback loops separated by a diode splitter. The integrator has two outputs and sums both charge and discharge current pulses. Rising and falling edge of the square wave causes exponential voltage spikes on the capacitors in the feedback loop. After a number of current pulses the voltage in the feedback loops is settled. The voltage values (with the opposite sign) from both outputs are summed in differential stage of instrumentation amplifier and then processed to digital form using 16-bit analog-to-digital converter.

The circuit differs from the classical charge-discharge circuit in using only one integrator in the demodulator. Demodulator with the diode splitter does not require the control, which makes it almost pure analog circuit (except for switching the gain). The elimination of analog switches simplifies the design. The circuit is immune to parasitic capacitances, similarly to the charge-discharge circuit. In the modified circuit the charge injection from analogue switches in not an issue.

The operating frequency of the classic circuit is limited by the speed of analog switches to a few megahertz. Unfortunately, the operating frequency of the modified system, despite the use of high-speed Schottky diodes, is also limited to a few megahertz. Operating frequency is limited by the speed of voltage rise at the output of operational amplifier, which has to switch between voltages on two capacitors in two feedback loops.

4. Summary

The paper presents two basic methods of measuring small capacitance used in electrical capacitance tomography: a frequency method with excitation using a sine wave and the charge-discharge method with excitation using a square wave. The modification of the charge-discharge method was also presented. The construction of the synchronous detector in these circuits was described.

In the charge-discharge method the synchronous detector is placed at the beginning of receiver channel. The charge injected by the analog switches is large comparing to the charge transferred through the measured capacitance. In effect this introduces the shift of the zero level.

Switch-less charge-discharge circuit is characterized by parameters, measurement uncertainty and speed, similar to the classic charge-discharge. The advantage of this circuit is a much simpler structure.

Several models of electrical capacitance tomograph were elaborated at our Division. The charge-discharge circuit was used in ET3 tomograph. The switch-less circuit was used in IREna tomograph. In the recent construction of our team – EVT4 tomograph – a single-shot high voltage (SSHV) circuit, which is another modification of charge-discharge circuit, was applied.

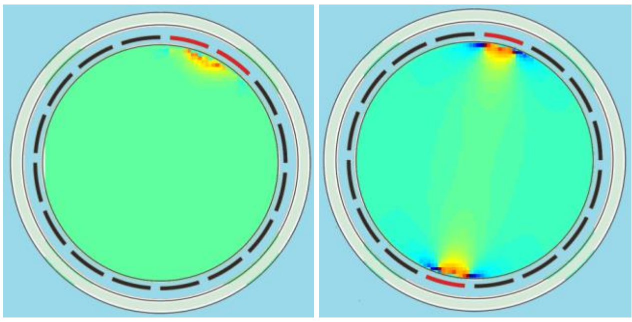

Fig. 1. 2D map of sensitivity of capacitance measurement on small change of permittivity in a small region of examined space. Sensitivity map in the cross section of cylindrical sensor with 16 electrodes for capacitance measurement for: pair of adjacent electrodes (left), pair of opposite electrodes (right)

Fig. 2. Measurements of mutual capacitance of electrodes of cylindrical, tomographic sensor with 12 electrodes in one ring. The characteristic U-shaped plot is obtained when one driving electrode is fixed and the others are sensing electrodes. Three U-shaped parts of the plot for three different driving electrodes is shown. The maximum value corresponds to a pair of adjacent electrodes, the lowest corresponds to pair of opposite electrodes

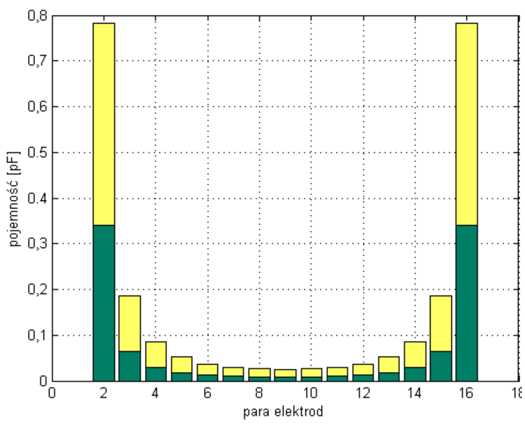

Fig. 3. Mutual capacitance of electrodes of cylindrical sensor (one ring, 16 electrodes) for pairs from 1-2 to 1-16. Values for the sensor filled with a material with a relative permittivity $\varepsilon_r = 3$ (yellow) and filled with air – $\varepsilon_r = 1$ (green)

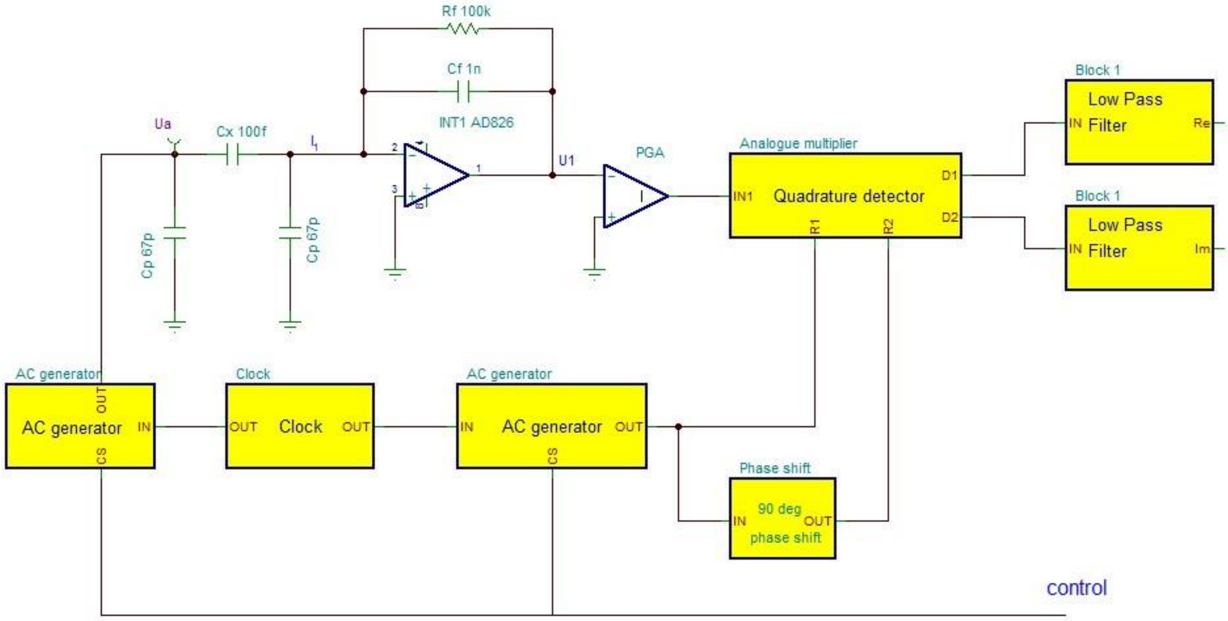

Fig. 4. Block diagram of the AC circuit with the quadrature demodulator for simultaneous measurement of capacitance and conductivity

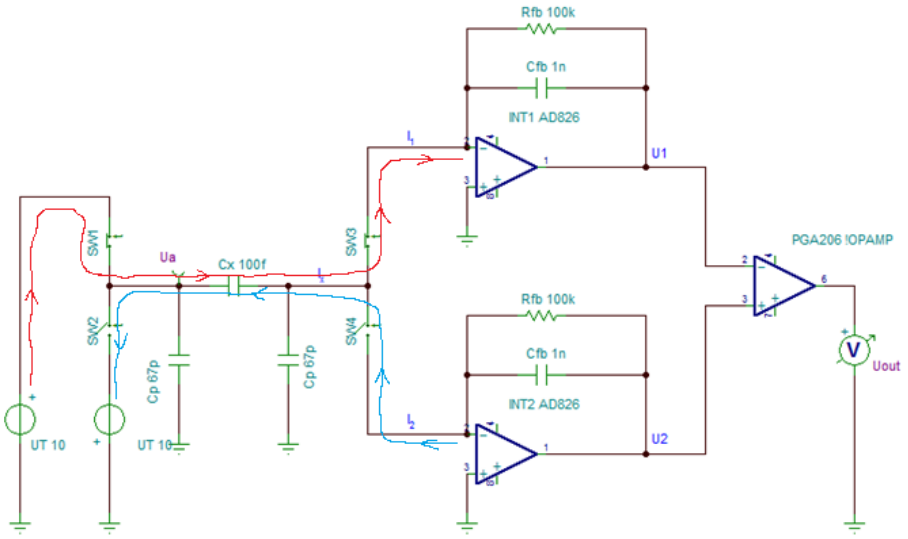

Fig. 5. Schematic diagram of the charge-discharge circuit. The path of current flow in charging and discharging phase is shown

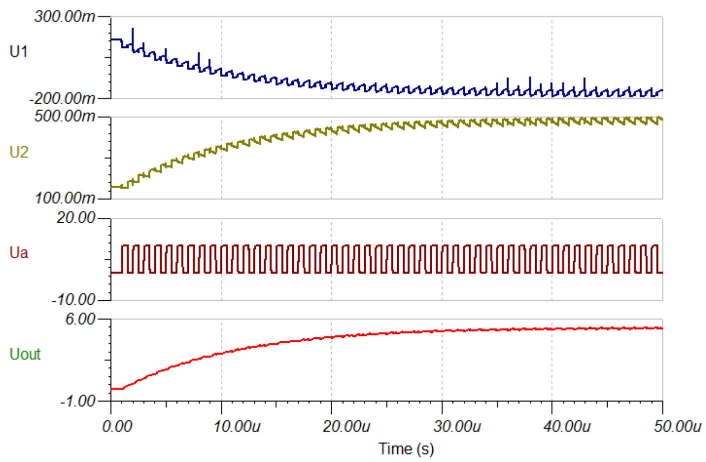

Fig. 6. Numerically simulated voltage waveforms in the charge-discharge circuit (stimulating voltage amplitude: U_A =10 V; U_1, U_2 – voltage at integrators output; U_{OUT} – voltage at output of instrumentation amplifier; measured capacitance C_X = 100 fF; elements in feedback loop: R_{FB} = 100 kΩ; C_{FB} = 470 pF; excitation frequency: f = 1 MHz)

 p-ISSN 2083-0157, e-ISSN 2391-6761

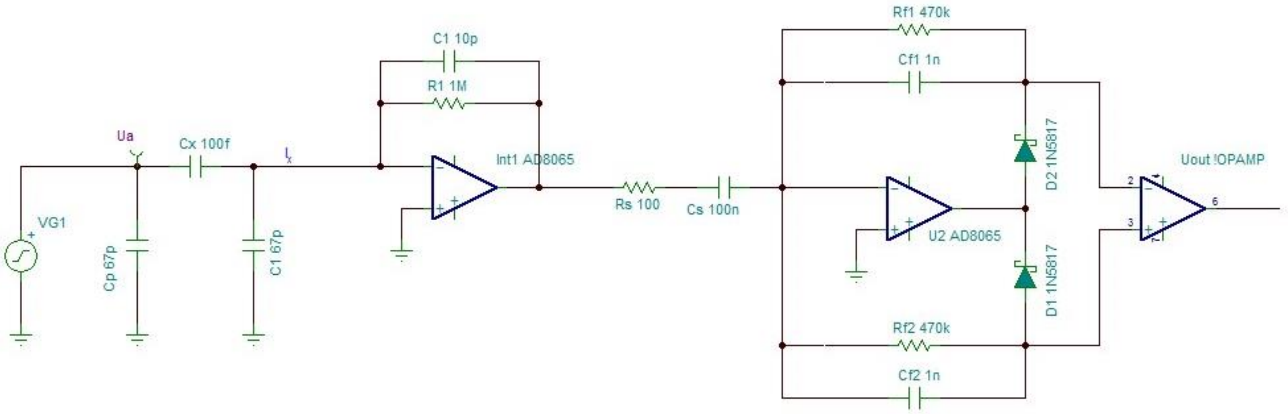

Fig. 7. Switch-less charge-discharge circuit with active rectifier and diode splitter

Bibliography

[1] Baxter L.K.; Capacitive Sensors: Design and Applications. IEEE Press Series on Electronics Technology, 1996.

[2] Brzeski P., Mirkowski J., Olszewski T., Pląskowski A., Smolik W., Szabatin R.: Multichannel capacitance tomograph for dynamic process imaging. Opto-Electronics Review, 2003, 175–180.

[3] Hu H., Katsouros M., Yang W.Q., Huang S.M.: Further analysis of charge/discharge capacitance measurement circuit used with tomography sensors. Sensors & Transducers Journal, 80(6)/2007, 1246–1256.

[4] Huang S.M., Plaskowski A.B., Xie C.G. & Beck M.S.: Capacitance-based tomographic flow imaging system. Electron. Lett., 24/1988, 418–419.

[5] Huang M., Stott A.L., Green R.G., Beck M.S.: Electronic transducers for industrial measurement of low value capacitances. J. Phys. E: Sci. Instrum., 21/1988, 242–250.

[6] Huang S.M., Xie C.G., Thorn R., Snowden D., Beck M.S.: Design of sensor electronics for electrical capacitance tomography. IEE Proceedings-G, 139(1)/1992, 83–88.

[7] Kryszyn J., Smolik W., Radzik B., Olszewski T., Szabatin R.: Switchless Charge-Discharge Circuit for Electrical Capacitance Tomography. Meas. Sci. Technol. 25/2014, 115009 (9).

[8] Lionheart W. R.: EIT reconstruction algorithms: pitfalls, challenges and recent developments. Physiol. Meas., 25/2004, 125–142.

[9] Plaskowski A., Beck M., Thorn R., Dyakowski T.: Imaging industrial flows. Applications of electrical process tomography, IOP Publishing Ltd, 1995.

[10] Reinecke N., Mewes D.: Recent developments and industrial research applications of capacitance tomography. Meas. Sci. Technol., 7/1996, 325–337.

[11] Smolik W., Mirkowski J., Olszewski T., Radomski D., Brzeski P., Szabatin R.: Measurement circuit based on programmable integrators and amplifiers for electrical capacitance tomography, Kwartalnik Elektroniki i Telekomunikacji, 51/2005, 127–137.

[12] Smolik W.T., Olszewski T., Radzik B., Szabatin R.: Switch-Less Charge-Discharge Circuit for Electrical Capacitance Volume Tomograph ET4. 6th International Symposium on Process Tomography. Cape Town, RPA, 2012.

[13] Yang W.Q., Stott A.L., Beck M.S., Xie C.G.: Development of capacitance tomographic imaging systems for oil pipeline measurements. Rev. Sci. Instrum., 66/1995, 4326–4332.

[14] Yang W.Q.: Hardware design of electrical capacitance tomography systems. Meas. Sci. Technol., 7/1996, 225–232.

[15] Yang W.Q., York T.A.: New AC – based capacitance tomography system. IEE Proc-Sci. Measurement Technology, 146(1)/1999, 47–53.

Prof. Waldemar Tomasz Smolik
e-mail: W.Smolik@ire.pw.edu.pl

Waldemar T. Smolik received the M.Sc., the Ph.D. and D.Sc. degree in electronics engineering from Warsaw University of Technology, Warsaw, Poland in 1991, 1997 and 2014, respectively. Since 2014, he is an Associate Professor at the Institute of Radioelectronics and Multimedia Technology, Electronics and Information Technology Faculty, Warsaw University of Technology. He is the head of the Laboratory of Electronics Application in Nuclear Medicine at the Division of Nuclear and Medical Electronics. His main research interests are computer engineering, computed tomography and medical imaging. He has published over 70 scientific papers.

M.Sc. Eng. Jacek Kryszyn
e-mail: J.Kryszyn@ire.pw.edu.pl

Received the M.Sc. degree in electronics and computer engineering from Warsaw University of Technology, Warsaw, Poland in 2012. Ph.D. student and the Assistant with the Nuclear and Medical Electronics Division, Institute of Radioelectronics and, Electronics and Information Technology Faculty, Warsaw University of Technology. His field of interest covers Electrical Capacitance Tomography, especially simulations of the electric field and reconstruction of images.

M.Sc. Eng. Tomasz Olszewski
e-mail: T.Olszewski@ire.pw.edu.pl

Tomasz Olszewski received his M.Sc. in electronics from Warsaw University of Technology, Warsaw, Poland in 1982. He has been employed at the University since 1989, currently as a Senior Lecturer. His main interests cover analogue and digital electronics in impedance tomography. He is the main designer of ET and ET3 capacitance tomographs, developed at the Nuclear and Medical Electronics Division.

Ph.D. Eng. Roman Szabatin
e-mail: R.Szabatin@ire.pw.edu.pl

Roman Szabatin received the M.Sc. degree in electronics apparatus and the Ph.D. degree from Warsaw University of Technology, in 1972 and 1983, respectively. Since 1973, he has been with the Nuclear and Medical Electronics Division, Institute of Radioelectronics, Electronics and Information Technology Faculty, Warsaw University of Technology, as an Associate, Senior Associate, and Senior Scientist. His main research interests include nuclear and medical instrumentation and medical imaging (gamma cameras, SPECT and PET). He has published over 50 scientific papers.

otrzymano/received: 20.09.2016 *przyjęto do druku/accepted: 15.02.2017*